Applied Calibration and Validation Method of Dynamic Process Simulation for Crushing Plants

(article starts on next page)

Article

Applied Calibration and Validation Method of Dynamic Process Simulation for Crushing Plants

Kanishk Bhadani [1,*], Gauti Asbjörnsson [1], Barbara Schnitzer [2,3], Johannes Quist [4], Christian Hansson [5], Erik Hulthén [1] and Magnus Evertsson [1]

1   Department of Industrial and Materials Science, Chalmers University of Technology, SE-412 96 Göteborg, Sweden; gauti@chalmers.se (G.A.); erik.hulthen@chalmers.se (E.H.); magnus.evertsson@chalmers.se (M.E.)
2   Department of Mathematical Sciences, Chalmers University of Technology, SE-412 96 Göteborg, Sweden; barsch@chalmers.se
3   Department of Mathematical Sciences, University of Gothenburg, SE-412 96 Göteborg, Sweden
4   Computational Engineering and Design, Fraunhofer-Chalmers Centre, SE-412 88 Göteborg, Sweden; johannes.quist@fcc.chalmers.se
5   Region Berg och Asfalt, Skanska Industrial Solutions AB, SE-215 32 Malmö, Sweden; christian.hansson@skanska.se
*   Correspondence: kanishk@chalmers.se

Abstract: There is a need within the production industry for digitalization and the development of meaningful functionality for production operation. One such industry is aggregate production, characterized by continuous production operation, where the digital transformation can bring operational adaptability to customer demand. Dynamic process simulations have the ability to capture the change in production performance of aggregate production over time. However, there is a need to develop cost-efficient methodologies to integrate calibrations and validation of models. This paper presents a method of integrating an experimental and data-driven approach for calibration and validation for crushing plant equipment and a process model. The method uses an error minimization optimization formulation to calibrate the equipment models, followed by the validation of the process model. The paper discusses various details such as experimental calibration procedure, applied error functions, optimization problem formulation, and the future development needed to completely realize the procedure for industrial use. The validated simulation model can be used for performing process planning and process optimization activities for the crushing plant's operation.

Keywords: optimization; comminution; classification; digitalization; dynamic process; data-driven modeling; aggregate production

1. Introduction

Crushing and screening processes in aggregate production are intended to produce various sets of products based on size fraction. These products are used for different construction activities such as roads, railways, and infrastructure. Managing and operating a crushing plant to the need of market demands is a challenge for the industry, and there is a need for a digital support system for operators and managers of aggregate production processes. Despite the modeling and simulation development of the crushing plant [1–3], there are barriers within the industrial operation to use simulations for daily operation management. There is a constant need for maintenance of the validity of the underlying simulation model for the gradual changes occurring in the daily operations.

To address the need for increased functionality for the simulation environments to support daily operation, an optimization system for aggregate production is proposed, as shown in Figure 1 [4–6]. To make the decision based on the simulation model of equipment and process, referring to an aggregate crushing plant, there is a need to develop a calibration and maintenance routine for process simulation to derive useful and reliable

results from the optimization function [7–10]. Based on the choice of the equipment model in the process simulation, a continuous validation routine for effective use of the process simulation is required [6,11].
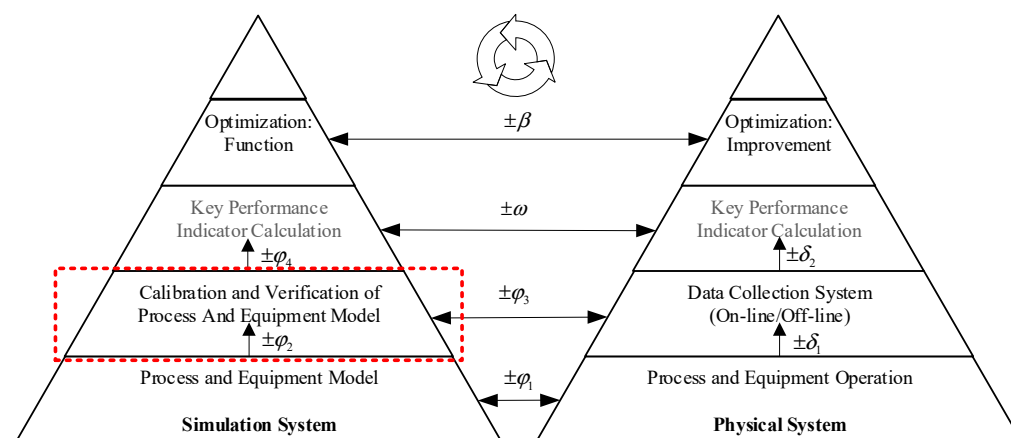
Figure 1. Error propagation model for the implementation of the optimization functionality in crushing plants [4].

This paper presents a methodological routine to calibrate and validate process simulations for industrial aggregate crushing plants (see Figure 1, red box). The application of an optimization method is presented to calibrate and tune equipment models based on the controlled data obtained from experimental design and survey. The applied optimization method uses an unconstrained gradient-based algorithm for calibration and tuning purposes, which is a computationally viable solution. This is followed by the configuration and validation of the dynamic process simulation based on mass flow data input, as captured during the controlled experiment.
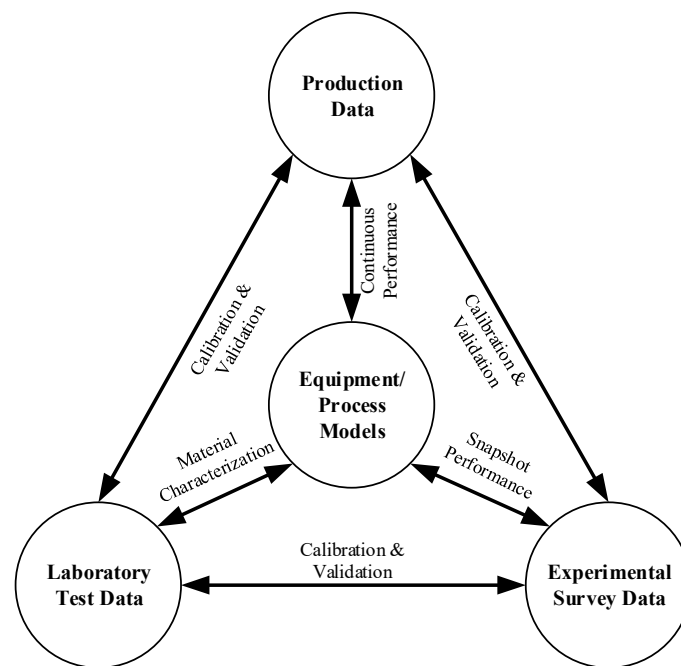
2. Process Modeling and Simulation Approach

There are various fidelities of models present for the comminution and classification equipment. For example, a crusher performance is described in detail by mechanistic principles by Evertsson [12], an empirical model by Whiten [13]. Similarly, multiple empirical, phenomenological, and mechanistic screen models are described by Karra [14], Whiten [15], and Soldinger [16,17], respectively. King [18] presented extensive work to demonstrate the need for using a reliable simulation model for improving crushing plant performance by using a case study of uranium production. The models are developed based on certain underlying assumptions on process stability and utilize both laboratory and industrial experimental data to be calibrated. With the current trends of increased transition to online data management systems and data analytics [19,20], the opportunity has emerged to utilize the existing knowledge within the models to adapt to the production data available. Alternatively, one can also approach the path of machine learning models to capture the behavior of the process performance using continuous time-series data (production data), as demonstrated by Li et al. [21,22].

The development in the dynamic process simulation for crushing plants [1,23] provides opportunities to integrate equipment models into the continuous process performance estimations. Integration of calibration methodologies for the dynamic process models to the digital data collection system such as mass flow and power draw can be a powerful and cost-efficient tool. The integration between the dynamic process simulation and on-line data capturing techniques can eliminate or reduce expensive survey sampling and laboratory test work. To address the abovementioned gaps, there is a need for developing methodologies that can support such system integration.

Figure 2 represents a schematic view of the pillars for the model calibration for equipment and process simulation applicable for the crushing plants. The laboratory data refer

to the material characterization data obtained by carrying out standard material tests, for example, material density, compressive stress, moisture content, breakage, etc. The experimental survey data refer to the controlled experiments performed at the crushing plant site using full-scale equipment to collect belt-cut samples for mapping equipment performance. This provides a snapshot indication of the process and equipment performance. The production data refer to the controlled data collected from the process plant operation, such as mass flow, power, process setpoints, and control signals. This delivers continuous data based on the complete operation of the plant, which is influenced by more than one equipment behavior. The transformation of the existing mechanistic or phenomenological models to use and adapt to different data sources needs computationally efficient optimization methods to fit the model to the data. There is a need to re-clarify the assumptions based on the selected model type.

Figure 2. Generalized view on the model and process calibration based on the sources of data.

2.1. Dynamic Process Simulation

The dynamic process modeling approach used in this study is based on the work by Asbjörnsson [1], and the process model is configured in MATLAB/Simulink environment. This modeling approach can capture discrete and gradual changes occurring in the physical crushing plant operation, such as delays in material flow, start-up sequence, discrete events, and wear. Each equipment model is based on the mathematical description of mass m and properties γ in a derivative form with respect to time, as shown in Equations (1) and (2).

$$\frac{dm(t)}{dt} = (\dot{m}_{i,in}(t) - \dot{m}_{j,out}(t)) \tag{1}$$

$$\frac{d\gamma_i(t)}{dt} = \frac{\dot{m}_{i,in}(t)}{m(t)}(\gamma_{i,in}(t) - \gamma_i(t)) \tag{2}$$

The material flow is regulated using interlocks and regulatory controllers. The lag and response of the process operation due to the hold up of material in equipment such as conveyor and feeder is described by Equations (3) and (4), where t is the current time step, θ is the delay time, τ is a time constant, K is a steady-state process gain, $u(t)$ is the input parameters, and $y(t)$ is the system output.

$$y(t) = u(t - \theta) \tag{3}$$

$$\tau\frac{dy}{dt} + y(t) = Ku(t) \tag{4}$$

2.2. Crusher Model

The model used for the crusher is a fast mechanistic model based on Evertsson [12] and implemented into dynamic simulation by Asbjörnsson et al. [24]. Figure 3 represents an overview of the interface of the crusher model. The model uses inputs such as material feed stream (consisting of material properties, product size distribution, and mass flow), crusher geometrical design and setting, material breakage, selection characterization, and flow characterization. The model is called fast as compared to the full-scale mechanistic model [12], as the recursive calculation of the flow model of the dynamic material interaction with the geometry is simplified with user-defined input (e.g., fixed compression number). Furthermore, the force resolution for predicting pressure and corresponding power calculation is simplified with the Bond equation [25].
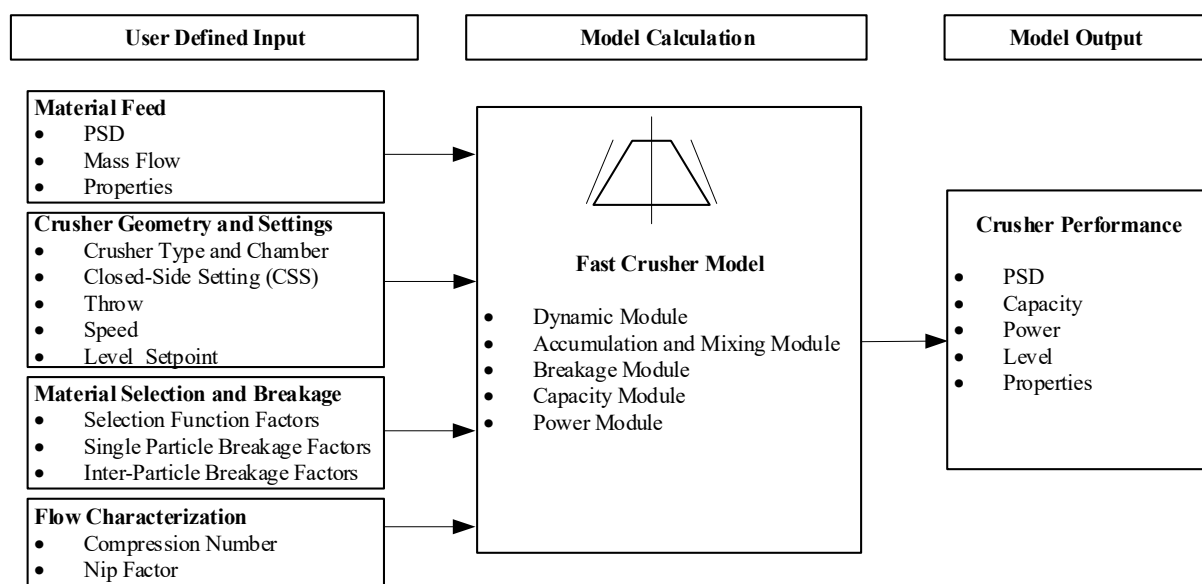

Figure 3. Overview of the fast-mechanistic crusher model implemented in Matlab/Simulink environment.

The property changes after each compression are sequentially calculated based on the defined compression zones using the input from the dynamic module; see Figure 4. The selection (S) and breakage (B) functions are based on the nominal response of the compression tests carried out for a particular material type [12].
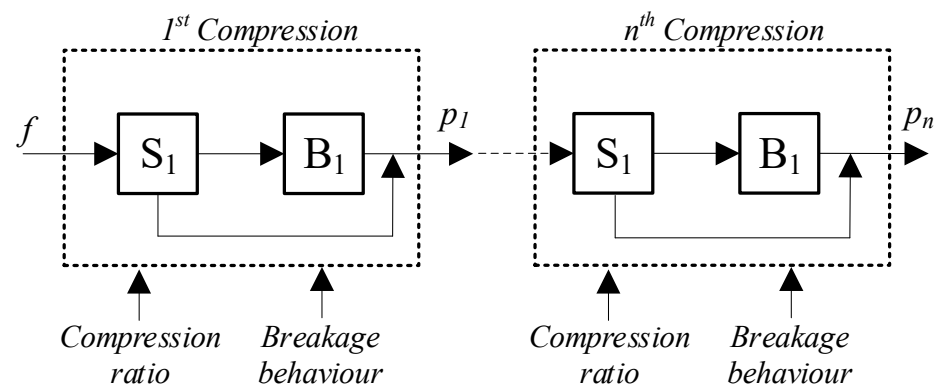

Figure 4. Schematic representation of the crusher model [5,12].

2.3. Screen Model

The screen model used is based on the Whiten [15] expression (Equation (5)), and a simplified model interface is shown in Figure 5. The model uses inputs such as material feed stream, screen geometrical design and settings, model parameter (separation size and sharpness), and outputs the separated material streams. Equation (5) represents the reduced partition curve (E_{oa}) to calculate the oversize material stream, where α is the sharpness of the separation, d_i is the geometric mean of the size interval i, d_{50} is the separation size, E is the efficiency at the screen aperture, and A is the screen aperture. In this work, the survey data are used to back-fit the model parameter and tune the screen aperture based on the noted data. A modification in the α parameter is applied where the value of the α is linearly dependent on the mass flow stream to capture the effect of different loading conditions with respect to the partition of the stream.

$$E_{oa} = \frac{\exp(\alpha x_i) - 1}{\exp(\alpha x_i) + \exp(\alpha) - 2}$$

$$x_i = \frac{d_i}{d_{50}}$$

$$d_{50} = \frac{\alpha A}{\ln\left[\left(\frac{100}{100-E} - 1\right)\exp(\alpha) + \left(\frac{100}{100-E} - 1\right) - 2\right]}$$
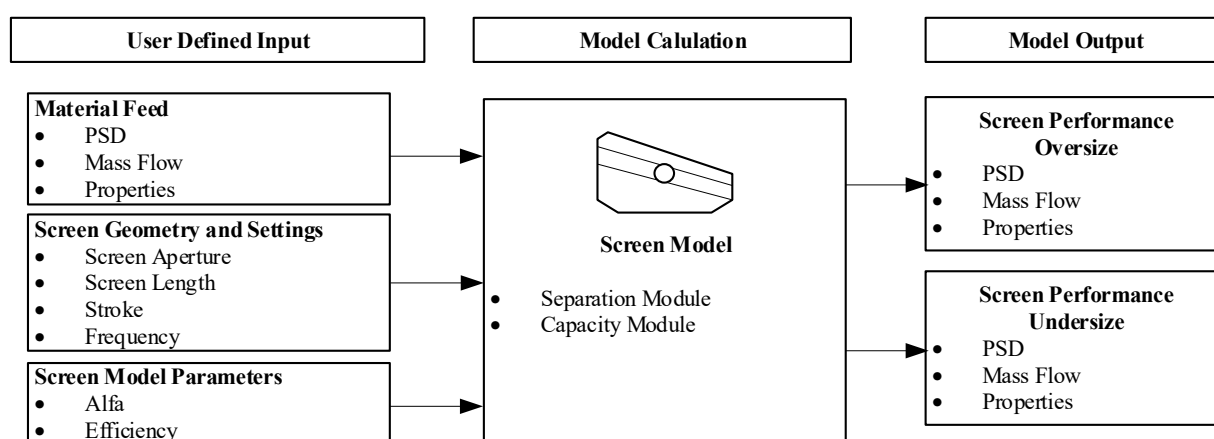
(5)

Figure 5. Overview of the screen model implemented in Matlab/Simulink environment.

3. Applied Experimental Method Description

A systematic method is applied to calibrate a full-industrial scale crushing plant using physical experimentation and validated using production data. The methodology consists of multiple steps, which include process mapping, experimental design, and data collection, with a physical survey leading to laboratory data and production data. This is followed by an applied optimization method for equipment calibration and validation of the process simulation.

3.1. Process Mapping

Figure 6 shows the tertiary crushing process stage of an aggregate production site in Sweden. The circuit consists of an H36 crusher followed by two consecutive double-deck screens producing four sellable products. The equipment is interconnected with conveyors which have mass flow measurement units installed. The mass flow units are also connected to cloud-based data storage. The plant is manually controlled by operating the crusher with the operator-defined settings, and the mass flow of the fresh feed (CV2) from the stockpile is manually regulated.
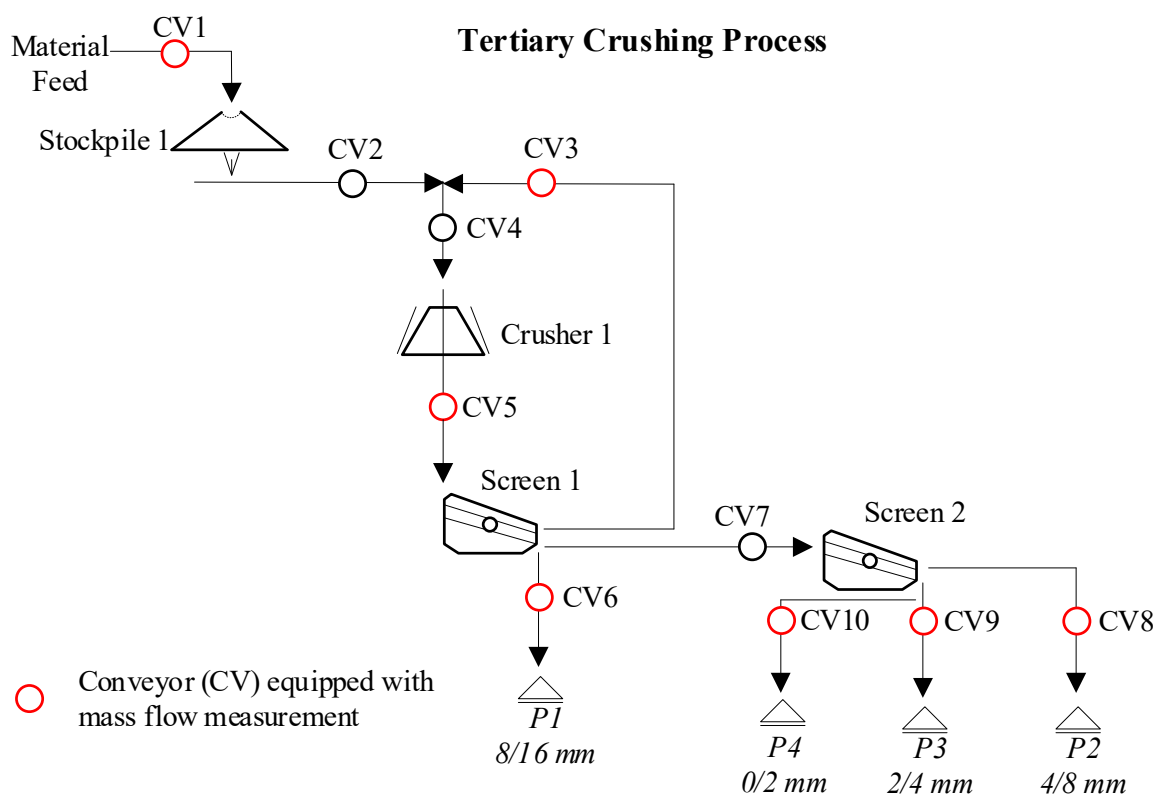
Figure 6. Tertiary crushing process for an industrial-scale aggregate production plant.

3.2. Experimental Design and Data Collection

To map the performance of the crusher, screens and process, an experimental design was applied, as shown in Figure 7. The details of the observed process settings and belt-cut points are shown in Table 1.
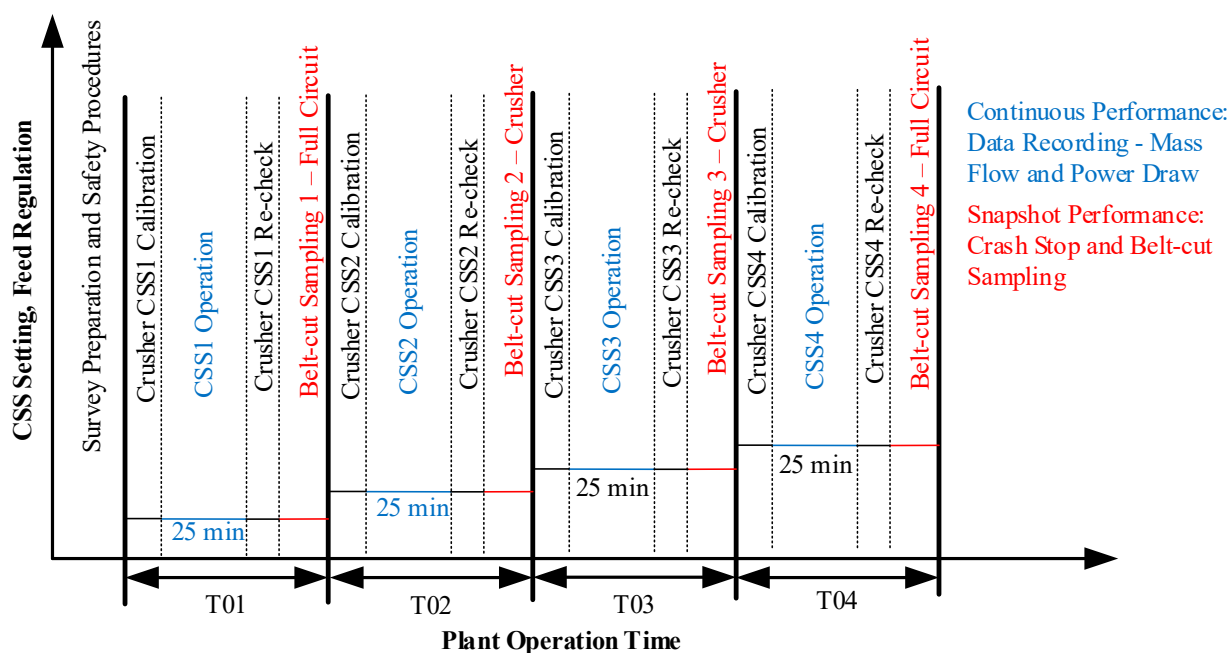

Figure 7. Experimental sequence applied for mapping the circuit performance of the crushing plant.

**Table 1.** Experimental noted values for the crushing plant.

Test ID	CSS Setpoint (mm)	CSS Calibration (mm)	CSS Re-Check (mm)	Operation Time (min)	Belt-Cut Sampling Point
T01	12	11.5	12.5	25	CV (3, 4, 5, 6, 7, 8, 9,10)
T02	15	15	15	25	CV4, CV5
T03	17	16.5	17.5	25	CV4, CV5
T04	19	18	19	25	CV (3, 4, 5, 6, 7, 8, 9,10)

- A series of four experiments were performed consisting of crusher closed-side setting (CSS) calibration, crusher operation, crusher CSS re-check, followed by a crash stop of the circuit for belt-cut sampling. The rationale behind the chosen incremental crusher set points is based on the type of crusher, top size particle in incoming feed, and the practical possibility of operation. The crusher CSS was calibrated and re-checked using hard clay to observe the deviation in the setting before and after the continuous operation.

- Continuous operation of the crusher at the choke feed condition and steady-state process condition was performed to capture continuous data for mass flow. The crusher was operated for 25 min to be able to capture a minimum of 20 min of the steady-state performance condition.

- The circuit was crash-stopped to perform the belt-cut sampling at various conveyor points based on the experimental plan. For all four test runs, crusher feed and product were sampled. For the screen calibration, two experimental tests (T01 and T04) captured the belt cut samples for screen feeds and products. The rationale behind choosing these two tests was to capture the screens' performance at two loading conditions: low CSS (T01) created a high load on screen 2 (high generation of fine material), while high CSS (T04) created a high loading condition in screen 1 (high generation of coarse material).

- The belt-cut sampling lengths (1–3 m) were selected based on the top size of material on the conveyor, uniformity of material distribution, and material weight required to achieve statistical significance based on top size [15,26]. The samples were limited to include replicates. Sieving analysis was performed on each sampled material using SS-EN 933-1:2012 standard [26]. For the survey data, a basic check was performed if the data set was in line with the knowledge of the equipment. For example, opening the CSS of the crusher should lead to increased production of coarse products.

3.3. Applied Optimization Method

Based on the sieving analysis on the belt-cut sampled material at various settings, an optimization method is applied to fit the model to the data. An illustration of the applied calibration and validation process is demonstrated in Figure 8. In particular, the crusher and screen models are calibrated to the experimental belt-cut data for which the detailed optimization problem formulation is presented. The optimization problems formulations presented for crusher and screen are solved using an unconstrained gradient-based approach, the Quasi-Newton Method [27]. The advantage of using this approach is that it is computationally efficient, although it can be sensitive to the start point if multiple local minima exist. To address the limitation with the local minima, the optimization problems were solved at multiple combinations of start-points to obtain the optimizer and optimum value. The solution sets were evaluated based on the optimum values (sorted with lower values) and corresponding optimizer values. For low optimum value solutions, the optimizers were compared, and if they were found to be in close vicinity of other similar solutions, the local minima were regarded as representing global minima. The application at this stage is limited to evaluate the sensitivity of the optimizer to the optimum value.
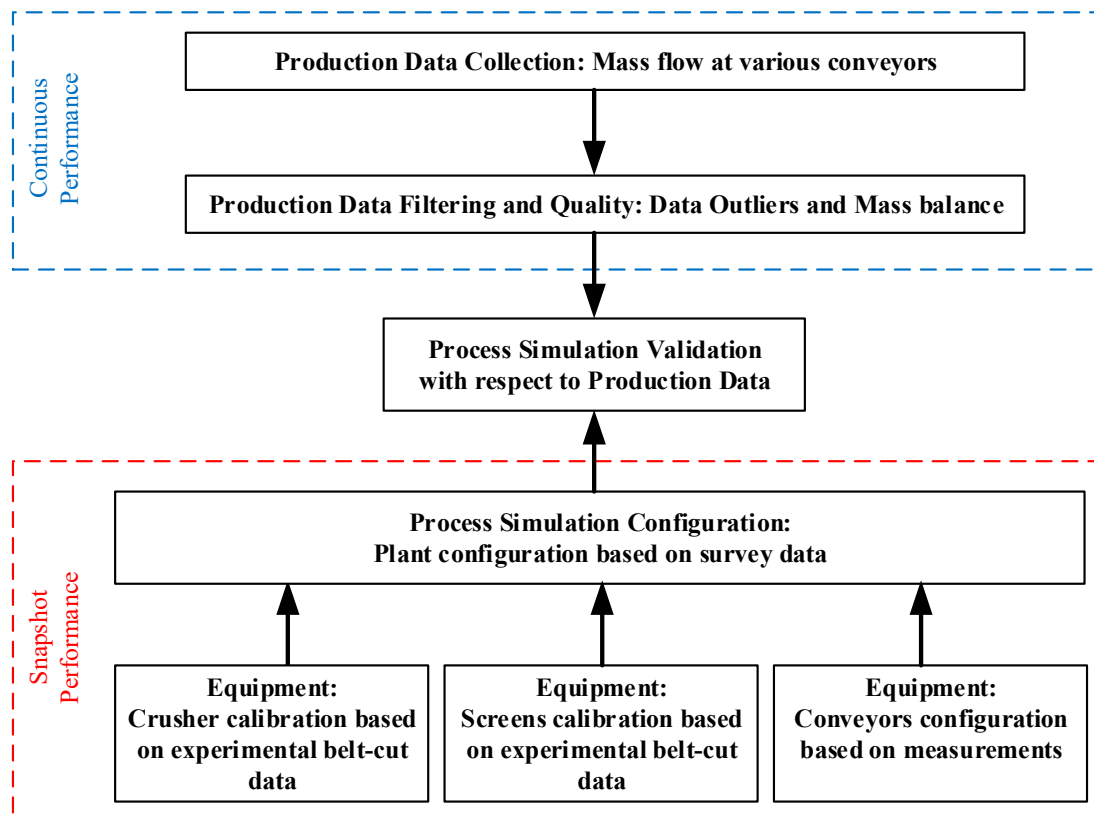
Figure 8. The steps for calibration and validation of dynamic process simulation of the crushing plant.

3.3.1. Crusher Optimization Problem Formulation

The crusher model is calibrated in two steps: Capacity Optimization and Product Size Distribution (PSD) Optimization. The fast-mechanistic model consists of 10 tuning variables (model parameters) corresponding to inter-particle breakage (x_1, x_2, x_3, x_4), single particle breakage (x_5, x_6, x_7, x_8), selection (x_9), and nipping angle (x_{10}). Depending on the choice of functions used inside each module in the model, the number of variables to be tuned can vary. The choice of the two sequential optimization problem formulations for the crusher is based on the representation of two distinct performance indicators (capacity and PSD) and their relationship with the model variables. In the Capacity Optimization (See Equation (6)), the objective function is to minimize the sum of the relative errors between the crusher-measured capacity (Cap_{Di}) and the simulated capacity (Cap_{Si}) for the n number of tested settings of *CSS*.

$$
\min \sum_{i=1}^{n} \left| \frac{(Cap_{Di} - Cap_{Si})}{Cap_{Di}} \right|
$$
$$
w.r.t \rightarrow x_k, [k = 10]
$$
$$
where,
$$
$$
[x_k]_0 = [1] \tag{6}
$$
$$
n = 4
$$
$$
Optimizer = x_k^*
$$

In the PSD Optimization for the crusher (See Equation (7)), the objective function is to minimize the weighted (w_j) sum of errors for the data ($PSDf_{Dji}$) and the simulation ($PSDf_{Sji}$) for the values of the n number of tested settings. The PSD values are in the frequency domain for the m number of given sieve sizes (**xsize**), and *mat* represents the nominal

material characterization values for a given material type. The PSD in the frequency and the cumulative domain is in fraction passing for the sieve size.

$$
\begin{aligned}
&\min \sum_{i=1}^{n} \sum_{j=1}^{m} w_j \left| (PSDf_{Dji} - PSDf_{Sji}) \right| \\
&w.r.t \rightarrow x_k, [k = 1, 2, \ldots, 9] \\
&where, \\
&[x_k]_0 = [1\ 1\ 1\ 1\ 1\ 1\ 1\ 1\ 1] \\
&n = 4,\ m = 25 \\
&Optimizer = x_k^* \cdot mat
\end{aligned}
\tag{7}
$$

The weighted function (w_j) is given in Equation (8), which is a function of the sieve size used in the simulation. The purpose of the weighted function is to steer and compensate for the distribution of the number of data points available at different sieve size ranges. The distribution is defined by the square root 2 series ranging from 63 μm to 360 mm. The function weighs higher on the coarse end of the particle size compared to the fine end of the particle size range. The weight on the smallest sieve size is set to 1 to prevent the tail of the sieve size from under compensating for the fine sieve size range. A graphical representation of w_j is shown in Figure 9.

$$
z_j = \log_2(xsize_j) + |\log_2(\min(\mathbf{xsize}))|
$$
$$
w_j = \begin{cases} z_j/(\max(\mathbf{z}))\forall(j = 1, 2, \ldots, 24) \\ 1, (j = 25) \end{cases}
\tag{8}
$$

where,

$\mathbf{xsize} = [360; 250; 125; 90; 63; 45; 31.5; 22.4; 16; 11.2; 8; 5.6; 4; 2.8; 2; 1.4; 1; 0.7; 0.5; 0.35; 0.25; 0.177; 0.125; 0.088; 0.063]$
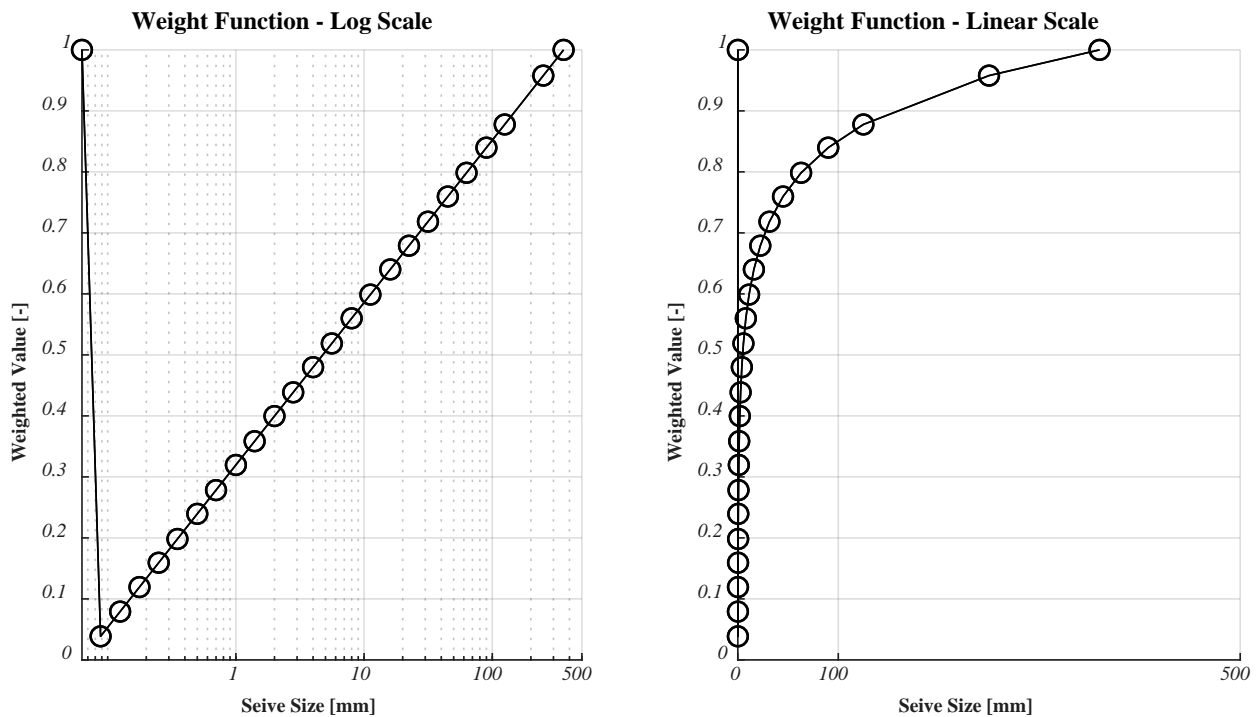

Figure 9. Graphical representation of the weighted function used in the optimization problem formulation.

3.3.2. Screen Optimization Problem Formulation

The screen model variables are tuned based on the objective to minimize the sum of errors between measured product size distribution ($PSDf_{Dji}$) and simulated product size distribution ($PSDf_{Sji}$) for p output material stream measured at n test settings for the m sieve sizes. Equation (9) presents a generalized optimization problem formulation for a double-deck screen. The aperture (A_d), efficiency at the aperture size (E_d), and sharpness parameter (α_d) are tuned based on the initial given values. The subscript d represents the notation for the position of the deck ($d = 1$ for Deck 1 and $d = 2$ for Deck 2).

$$\min \sum_{s=1}^{p} \sum_{i=1}^{n} \sum_{j=1}^{m} \left| \left((PSDf_{Dji})_s - (PSDf_{Sji})_s \right) \right|$$

$$w.r.t \rightarrow x_k, [k = 1, 2, \dots, 6]$$

$$where,$$

$$[\mathrm{x}_k]_0 = [\alpha_d, A_d, E_d] \forall d \tag{9}$$

$$n = 2, \ m = 25, p = 3$$

$$Optimizer = x_k^*$$

Depending on the loading condition of the screen, the sharpness parameter α_d is described as a linear function of the mass flow $m_{di}(t)$ for each screen deck (d) and the number of test settings (n); see Equation (10), where a_d and b_d are fitting parameters. In the case of an over-utilized screen, the sharpness parameter α_d can be assumed to also be dependent on the mass flow and product size distribution composition due to the changes in the incoming feed into the screen. In this case, the optimization problem shown in Equation (9) needs to be solved independently for each value of the test setting n.

$$\alpha_{di} = f(a_d, b_d) = a_d \cdot m_{di}(t) + b_d$$

$$i = 1, \dots, n \tag{10}$$

$$d = 1, 2$$

3.3.3. Production Data Collection and Filtering

The plant was equipped with load-cell sensors (*OJ1436 smart Belt Weigher Indicator*) for mass flow measurement at different conveyors (See Figure 6) [28]. The measurement accuracy is $\pm 1\%$ with normal maintenance according to the manufacturer's specification. The *OJ1436* calculates a new mass flow rate every 50 ms (20 Hz) and updates the total once per second (1 Hz) locally. This flow rate and total data are transferred to the online system (*smartTONNES*) once per minute (0.0167 Hz). The flow rate is transferred to the online system (average mass flow rate for the last minute based on the average of 60 readings) using an inbuilt router with an internet connection. The data for the plant were accessed using a custom-written code through API (Application Programming Interface). The data collected were post-processed to eliminate outliers (e.g., negative values, conveyor rated belt-scale values), and steady-state operation data were extracted. The mass balancing of the average data was checked for the different experimental settings. If the error was within the sensor variation, the data set was kept to the original; otherwise, data reconciliation could be performed.

4. Results

The results present the calibration of the crusher and screen models to the experimental belt-cut data. This is followed by the configuration and validation of the process simulation results against filtered production data.

4.1. Crusher Calibration

Figures 10 and 11 present the crusher calibration results for different tested CSS in the frequency domain and cumulative domain, respectively, for the optimization problem posed in Equation (7). The converged optimization solution resulted in an optimum value of 0.387 and an optimizer value of $x_{1\,to10}$ as 0.60, 0.30, −0.14, 0.64, 1.55, 0.83, −0.77, 0.75, 1.06, 0.80. The variables of the crusher model are found to be sensitive to the objective functions. It can be noted that the simulation is capable of representing the captured data. The weight function applied in the optimization problem formulation (see Equation (7)) helped to balance-fit the model well within the coarse operational region (sieve size above 2 mm), which is required for the aggregate process plant compared to the overfitting of the model in the fine region (sieve size below 2 mm) because of the multiple close-spaced data points. It was also found out that it was crucial to work with the frequency domain for optimization problem compared to the cumulative domain as the former avoid accumulated error in different sieve size data. In essence, the problem was decoupled for every sieve size fraction and test condition. The numerical application of the Quasi-Newton method for solving the optimization problem as an unconstrained gradient-based approach was found to be computationally efficient.
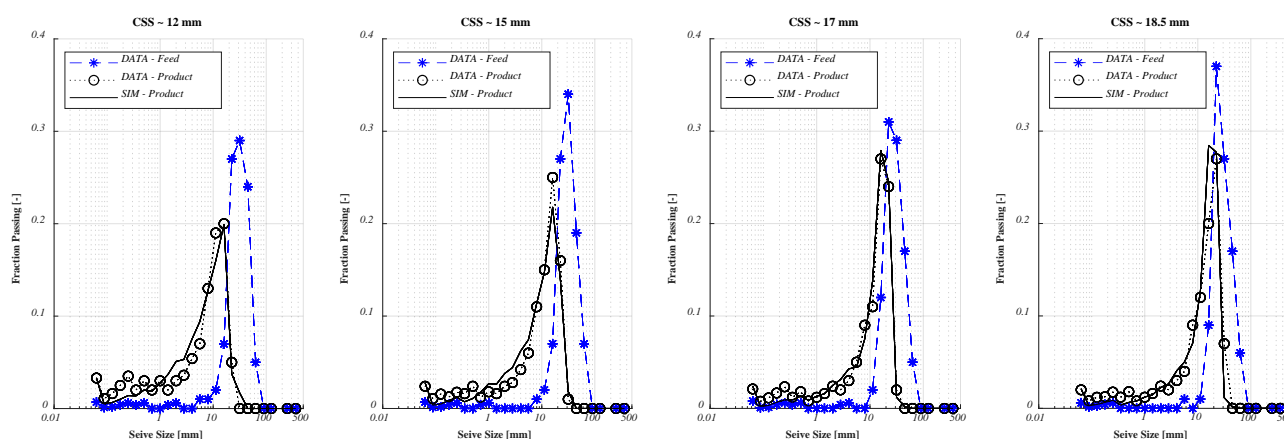

Figure 10. Crusher calibration result to the belt-cut experimental data in the frequency domain.
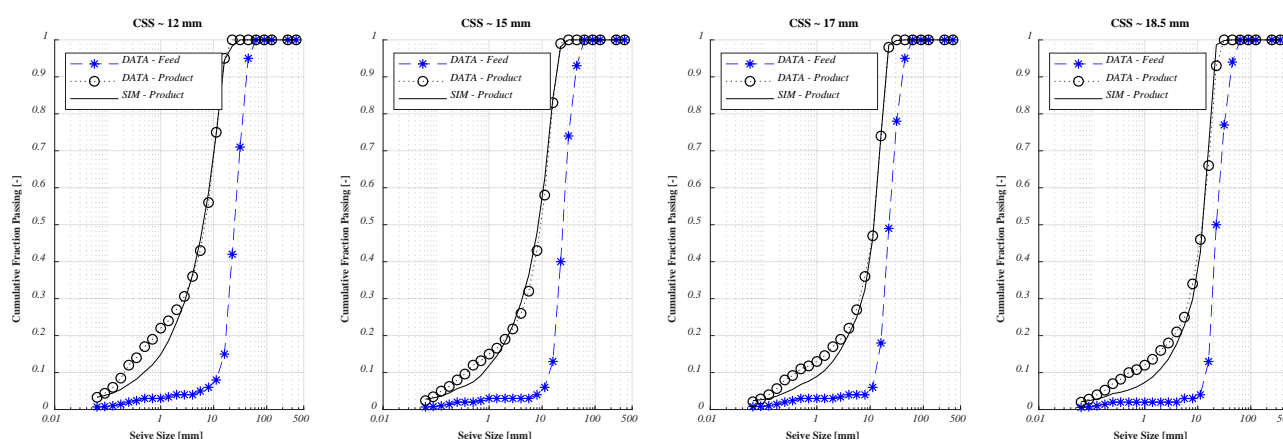

Figure 11. Crusher calibration result to the belt-cut experimental data in the cumulative domain.

4.2. Screen Calibration

Screen 1 was calibrated for each test load condition (T01 = 110 t/h and T04 = 134 t/h), and the parameter α was linearized to the mass flow for each deck in the double deck screen (See Equations (9) and (10)). Figure 12 presents the screen 1 calibration result for test conditions a) T01 and b) T04 in the cumulative domain. The optimizer values obtained

are $a_1 = -0.75$, $b_1 = 37.9$, $a_2 = -0.53$, $b_1 = 26.64$, $A_1 = 22.02$, $A_2 = 10.03$, $E_1 = 95$, and $E_2 = 95$. It was noted that the value of the aperture and efficiency at the aperture remained around the initial point while the variables associated with sharpness changed to fit the data due to the varied sensitivity of individual variables to the objective function.
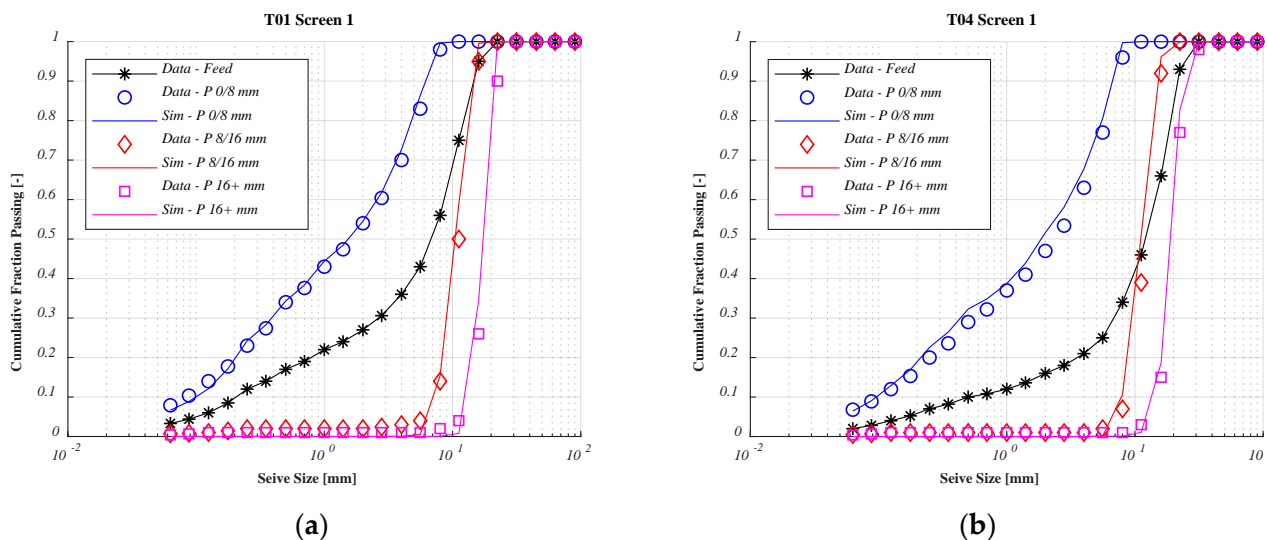

Figure 12. Screen 1 calibration results for (**a**) T01 and (**b**) T04 in the cumulative domain.

Screen 2 was calibrated for the combined test load condition (T01 = 54.66 t/h and T04 = 39.90 t/h) as per Equation (9). Figure 13 presents the screen 2 calibration result for test conditions a) T01 and b) T04 in the cumulative domain. The optimizer values obtained are $\alpha_1 = 9.30$, $\alpha_2 = 5.91$, $A_1 = 7.70$, $A_2 = 5.86$, $E_1 = 94.50$, and $E_2 = 94.69$. Both the calibrated results of the screen 1 and 2 models show satisfactory mapping to the data. However, it should be noted that the sampling for the screen performance using the experimental belt-cut method captures a snapshot of the screen performance. It was also noted that a discretization error could exist in the model, which is a function of the selected sieve size range. The fitting behavior of screen 1 (Figures A1 and A2) and screen 2 (Figures A2 and A4) calibration results for test conditions T01 and T04 in the frequency domain is presented in Appendix A.
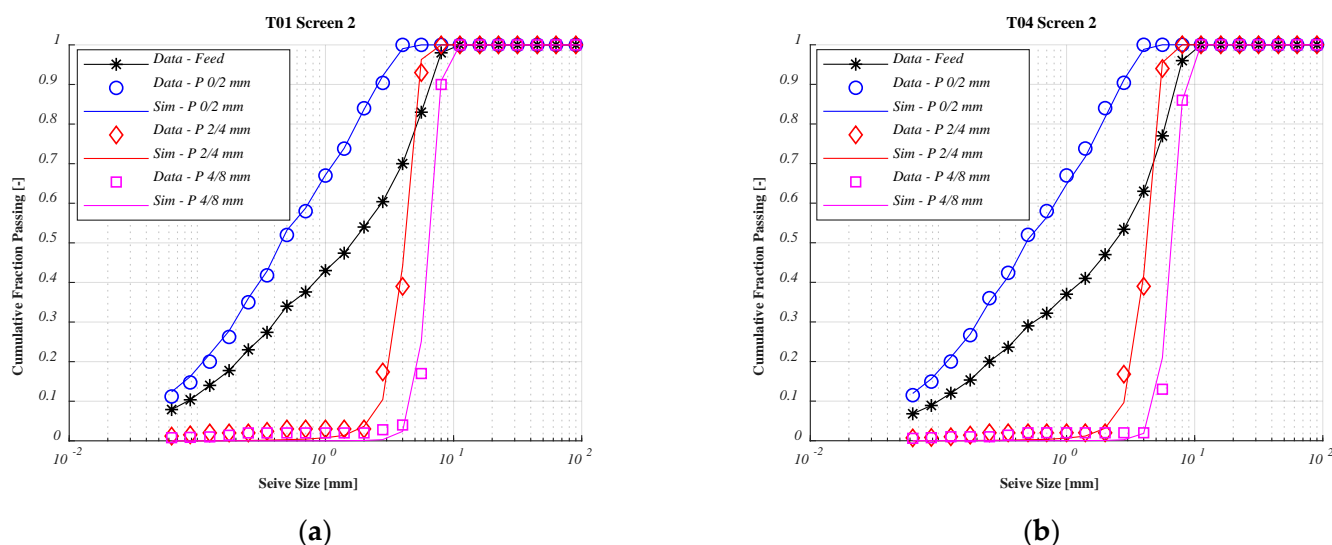

Figure 13. Screen 2 calibration results for (**a**) T01 and (**b**) T04 in the cumulative domain.

Figure 14 presents the partition curves for (a) screen 1 and (b) screen 2 (see Equation (5)). As mentioned earlier, the screening sharpness of screen 1 is dependent on the incoming mass flow, which is the function of the crusher product for the two-test condition (T01 and T04). T01 is the minimum setting in the crusher CSS, producing a high proportion of fines with low mass flow condition, while T04 is operating at maximum CSS, producing a low proportion of fines and higher mass flow. These two outputs first interact with the top deck of Screen 1, which results in screen performance variation with the loading condition. To further investigate this, the product quality of the screened material is plotted in Figure 15. It is evident from Figure 15a that the recirculating product (*P16+* mm) and product *P8/16* mm have a higher carryover of the oversize material from the test T01 compared to the test T04 condition, while the product *P0/8* mm has the vice versa response. This is the evidence where the two screening curves in Figure 14a are moving in the opposite direction with the loading condition change. On the contrary, the response of screen 2 is similar for both loading conditions (See Figures 14b and 15b). It can be noted that the product *P2/4* mm consists of a high proportion of undersize and oversize, which is a common phenomenon at this fraction size that can be caused due to screen clogging, wear, and moisture issues. The product is sometimes certified as *P2/5* mm depending on the market need and product quality.
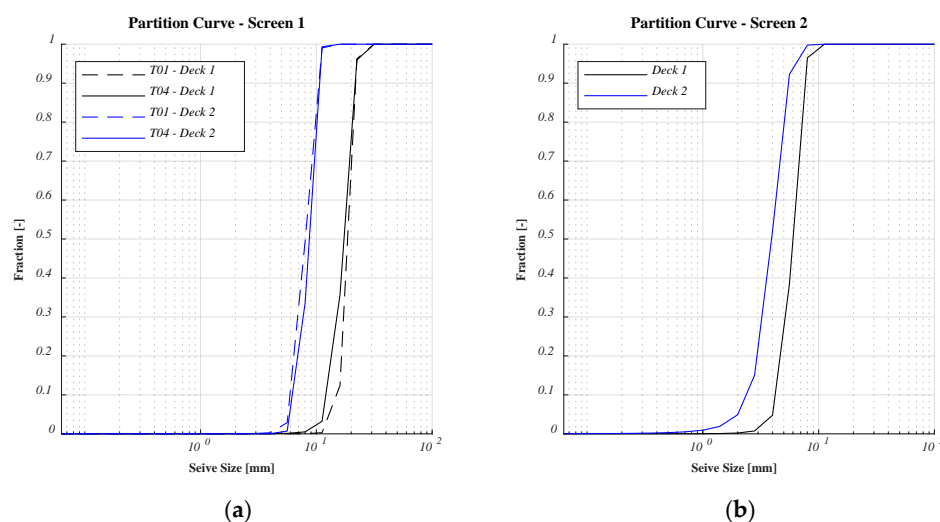

(a)　　　　　　　　　　　　　　　　　　　　(b)

Figure 14. Screening partition curves for the two screens. (**a**) Screen 1 and (**b**) Screen 2.
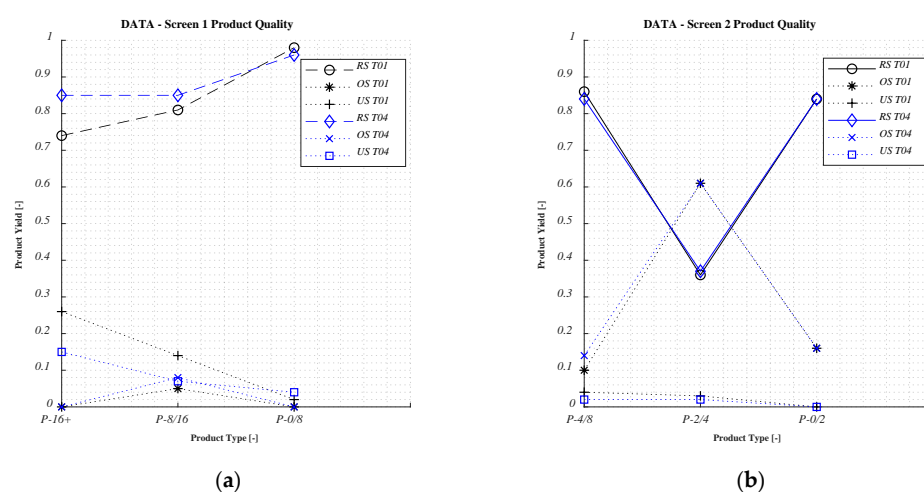

(a)　　　　　　　　　　　　　　　　　　　　(b)

Figure 15. Product quality of the screened products at different test conditions of (**a**) screen 1, (**b**) Screen 2, where RS—Regular Size, OS—Over Size, and US—Undersize for the particular product specification.

4.3. Process Validation

Figure 16 presents the comparison of various product streams from the dynamic process simulation to the production data captured from the mass flow system for the four test conditions (T01–T04: left to right). It can be observed that the process simulation captures the right trend, phase, and magnitude of the production for different product fractions, while certain discrepancies exist with the mass flow values.
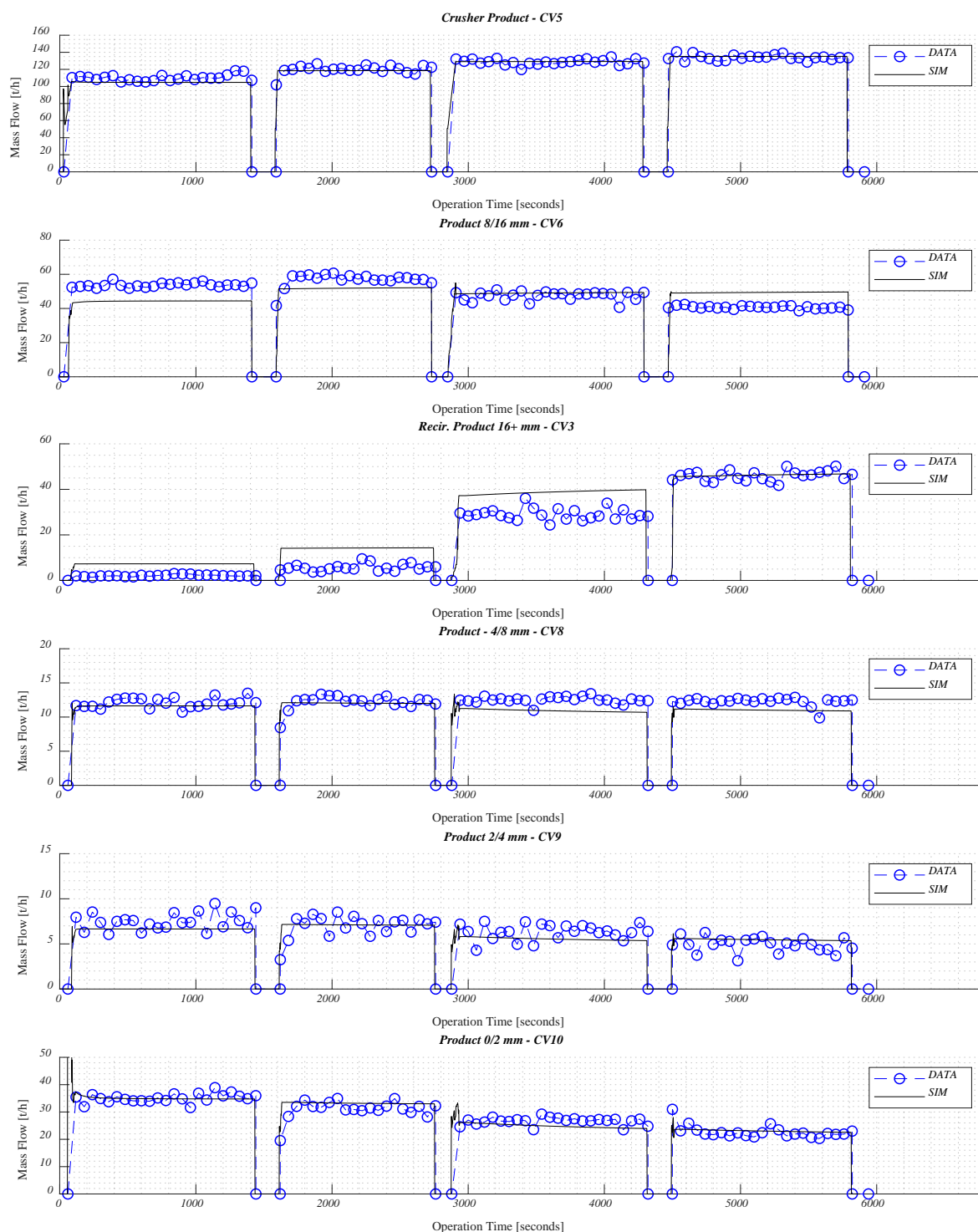
Figure 16. Dynamic simulation process results compared with the online production data for the four test conditions.

Table 2 presents the root mean square error (RMSE) values for each product stream and test condition. As can be noted from the RMSE, values are low for most cases, except Product *P8/16* mm and *P16+* mm. The origin of the error can be either associated with the crusher model, screen model, or production data. The crusher and screen models were calibrated to the snapshot performance captured from the experimental samples, and despite the controlled procedure, inherent variations exist in the process performance, which could result in such deviation. Up to 8–12% RMSE values, together with the visual scrutiny, have been shown to be acceptable for minerals processing application for a particular product flowrate [11]. Overall, the process performance prediction is satisfactory to use such models for process optimization and process planning for aggregate production.

Table 2. RMSE calculation between process simulation and production data.

Product Stream	T01	T02	T03	T04
Crusher Product	6.42	3.90	3.22	3.40
P8/16 mm	14.38	6.05	4.20	8.75
P16+ mm	5.10	8.40	11.38	7.72
P4/8 mm	2.56	0.70	1.77	1.48
P2/4 mm	2.06	0.78	1.28	1.01
P0/2 mm	1.90	2.42	2.22	1.50

Figure 17 presents product yield for different product streams obtained from experimental data of the absolute crusher performance compared to the values obtained from the production data. It can be commented that the dynamic screen performance is causing the difference between the values, especially at the coarser end of the products. To achieve a better production rate, it is important to consider both the crusher and screen process and their interaction effects, which can be simulated in a well-calibrated process simulation.
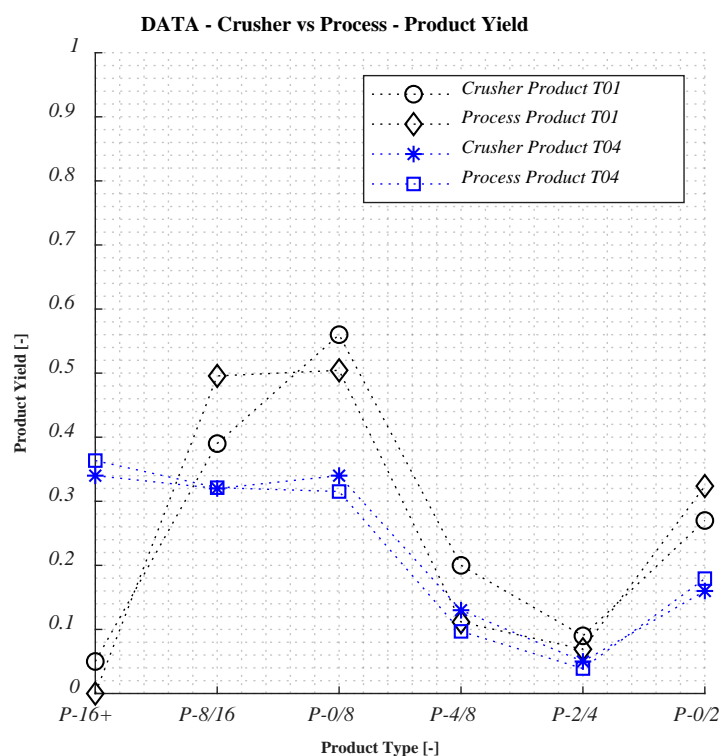
Figure 17. Product yield for different product streams obtained from data from crusher and process performance.

5. Discussion

The methodology for utilizing the existing model capabilities (crusher and screen) to adapt to the experimental data of an industrial scale crushing plant is shown. The use of mechanistic [12] or well-established phenomenological models [15] helps to generate knowledge about the equipment and process relations, rather than treating the process as a black-box system. This is needed to carry out process improvement and process optimization and interpret the appropriateness of the results for practical application. The operational strategy of the crushing plant operation can play an important role in the utilization of the dynamic process simulation capabilities. The plant under consideration was manually operated, which limited the inclusion of a feedback control loop in the process simulation.

Optimization problem formulation for product size distribution in the frequency domain is utilized for both the crusher and screen model, which resulted in a low error in model fitting. The choice of the optimization algorithm was based on the simplicity of the application, although other algorithms can also be applied to solve the defined problem. It is important to understand the sensitivity of each variable towards the output of the model as it helps in interpreting the optimization results in the model calibration. Usually, the algorithm is not supplied with the gradient values, and the gradient in the problem solution is estimated using numerical methods using the model response. One needs to be aware of these responses to understand optimizers in relation to the physical meaning of the model.

The experiment performed in this paper used two different sources of data (belt-cut samples and online production data) for calibration and validation of the process simulations. Knowing the limitation and applicability of the individual equipment model can pave the way to utilize the production data for the process calibration. The optimization problem can then be posed as a constrained-based optimization. This will be investigated to develop a method to calibrate the process simulation based on the production data (see Figure 8), which can further eliminate the costly experimental belt-cut sampling procedure. This development is needed for the easy use of the process simulation for industrial applications for daily operation. Further equipping the physical process with different sensors (power, mass flow, product size distribution) and connecting it to the cloud system for easy access are needed to completely utilize the benefits of the digital transformation. Further inclusion of the full-mechanistic crusher and screen model into the process simulation can lead to studies for the effect of major equipment level change (e.g., crusher liner, screen cloth) into production performance change.

6. Conclusions

A method consisting of controlled experimental design including belt-cut sampling together with the production data collection and application of an optimization approach to calibrate the dynamic process simulation for a crushing plant are presented. This was followed by validation of the process simulation with respect to the production data. A novel unconstrained optimization problem formulation for different crusher and screen models was presented. The use weighting function to generate a good fit of the crusher model was shown together with the application gradient-based algorithm (Quasi-Newton Method) to solve the optimization problem. The configured process model using calibrated equipment models was compared with the production data, which showed a low error value. The interaction effect between the crusher performance and screens performance was demonstrated, and one needs to consider a systems perspective to effectively utilize the process simulation capabilities.
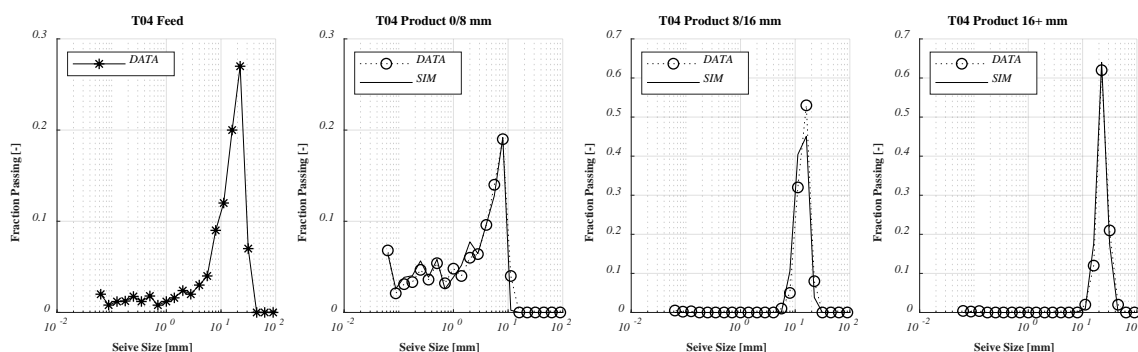
Appendix A

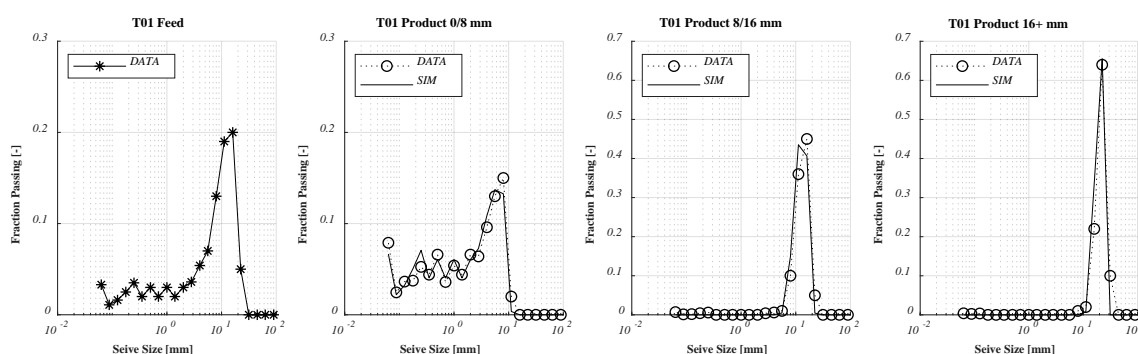**Figure A1.** Screen 1 calibration results for T01 in the frequency domain.

Figure A2. Screen 1 calibration results for T04 in the frequency domain.
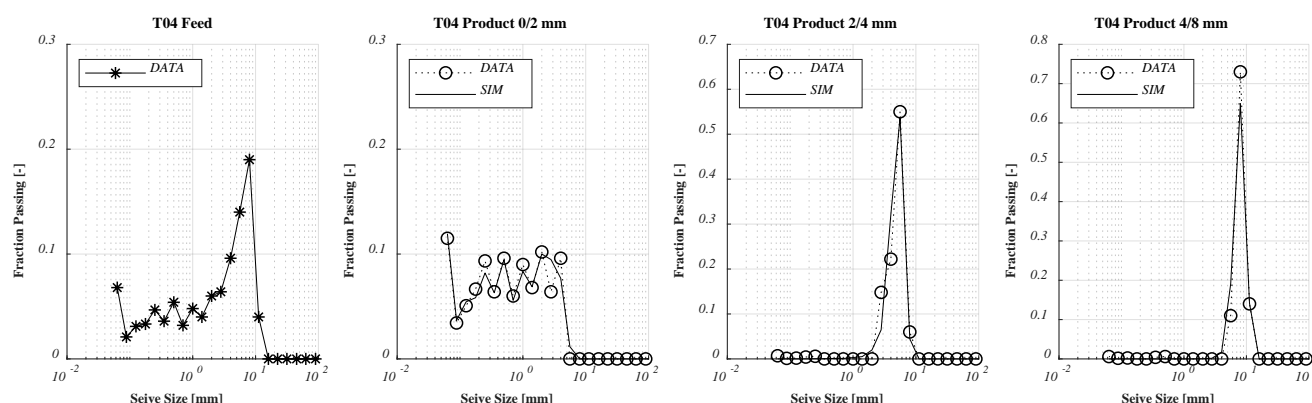
Figure A3. Screen 2 calibration results for T01 in the frequency domain.
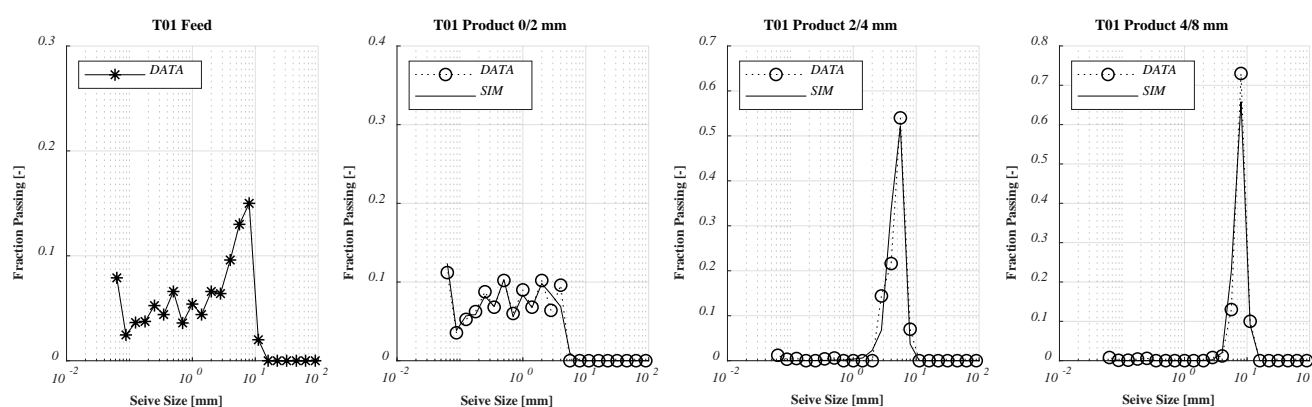

Figure A4. Screen 2 calibration results for T04 in the frequency domain.

References

1. Asbjörnsson, G. *Crushing Plant Dynamics*; Chalmers University of Technology: Gothenburg, Sweden, 2015.
2. King, R.P. *Modeling and Simulation of Mineral Processing Systems*; Elsevier Science: Amsterdam, The Netherlands, 2001.
3. Yamashita, A.S.; Thivierge, A.; Euzébio, T.A. A review of modeling and control strategies for cone crushers in the mineral processing and quarrying industries. *Miner. Eng.* **2021**, *170*, 107036. [CrossRef]
4. Bhadani, K.; Asbjörnsson, G.; Hulthén, E.; Hofling, K.; Evertsson, M. Application of Optimization Method for Calibration and Maintenance of Power-Based Belt Scale. *Minerals* **2021**, *11*, 412. [CrossRef]
5. Bhadani, K.; Asbjörnsson, G.; Hulthén, E.; Evertsson, M. Development and implementation of key performance indicators for aggregate production using dynamic simulation. *Miner. Eng.* **2020**, *145*, 106065. [CrossRef]
6. Bhadani, K. *Optimization Framework for Crushing Plants*; Chalmers University of Technology: Gothenburg, Sweden, 2019.
7. Huband, S.; Barone, L.; Hingston, P.; While, L.; Tuppurainen, D.; Bearman, R. Designing Comminution Circuits with a Multi-Objective Evolutionary Algorithm. In Proceedings of the 2005 IEEE Congress on Evolutionary Computation, Scotland, UK, 2–5 September 2005; pp. 1815–1822.
8. Huband, S.; Tuppurainen, D.; While, L.; Barone, L.; Hingston, P.; Bearman, R. Maximising overall value in plant design. *Miner. Eng.* **2006**, *19*, 1470–1478. [CrossRef]
9. Bhadani, K.; Asbjörnsson, G.; Hulthén, E.; Evertsson, M. Application of multi-disciplinary optimization architectures in mineral processing simulations. *Miner. Eng.* **2018**, *128*, 27–35. [CrossRef]
10. Bhadani, K.; Asbjörnsson, G.; Hulthén, E.; Bengtsson, M.; Evertsson, M. Comparative Study of Optimization Schemes in Mineral Processing Simulations. In Proceedings of the XXIX International Mineral Processing Congress, Moscow, Russia, 17–21 September 2018.
11. Brown, R.P.; Steyn, C.W.; Fouchee, R.J. Improving crusher performance by comparing various control strategies using a validated simulation. In Proceedings of the Comminution 2016, Cape Town, South Africa, 11–14 April 2016.
12. Evertsson, C.M. *Cone Crusher Performance*; Chalmers University of Technology: Gothenburg, Sweden, 2000.
13. Whiten, W.J. The simulation of crushing plants with models developed using multiple spline regression. *J. South. Afr. Inst. Min. Metall.* **1972**, *72*, 257–264.
14. Karra, V.K. Development of a model for predicting the screening performance of a vibrating screen. *CIM Bull.* **1979**, *72*, 167–171.

15. Napier-Munn, T.J.; Morrell, S.; Morrison, R.D.; Kojovic, T. *Mineral Comminution Circuits: Their Operation and Optimisation*; Julius Kruttschnitt Mineral Research Centre, The University of Queensland: Indooroopilly, Australia, 1996.
16. Soldinger, M. *Screening of Crushed Rock Material*; Chalmers University of Technology: Gothenburg, Sweden, 2002.
17. Asbjörnsson, G.; Bengtsson, M.; Hulthén, E.; Evertsson, M. Model of banana screen for robust performance. *Miner. Eng.* **2016**, *91*, 66–73. [CrossRef]
18. King, R.P. Simulation—The modern cost-effective way to solve crusher circuit processing problems. *Int. J. Miner. Process.* **1990**, *29*, 249–265. [CrossRef]
19. Qi, C.C. Big data management in the mining industry. *Int. J. Miner. Met. Mater.* **2020**, *27*, 131–139. [CrossRef]
20. Kusiak, A. Smart manufacturing. *Int. J. Prod. Res.* **2017**, *56*, 508–517. [CrossRef]
21. Li, H.; Evertsson, M.; Lindqvist, M.; Hulthén, E.; Asbjörnsson, G.; Bonn, G. Dynamic modelling of a SAG mill—Pebble crusher circuit by data-driven methods. In Proceedings of the SAG Conference 2019, Vancouver, BC, Canada, 22–26 September 2019.
22. Li, H.; Evertsson, M.; Lindqvist, M.; Asbjörnsson, G. Isolating the impact of pebble recycling on AG/SAG circuit: A data-driven method. In Proceedings of the 12th International Comminution Symposium, Online, 27–30 April 2020.
23. Asbjörnsson, G.; Evertsson, M.; Tavares, L.M.; Mainza, A.; Yahyaei, M. Different Perspectives of Dynamics in Comminution Processes. In Proceedings of the 12th International Comminution Symposium (Comminution '21), Cape Town, South Africa, 27–30 April 2020.
24. Asbjörnsson, G.; Hulthén, E.; Evertsson, M. Modelling and simulation of dynamic crushing plant behavior with MAT-LAB/Simulink. *Miner. Eng.* **2013**, *43*, 112–120. [CrossRef]
25. Bond, F.C. Third theory of comminution. *Min. Eng.* **1952**, *4*, 484.
26. SIS. *Tests for Geometrical Properties of Aggregates—Part 1: Determination of Particle Size Distribution—Sieving Method*; Swedish Standards Institute, SIS Förlag AB: Stockholm, Sweden, 2012; SS-EN 933-1:2012.
27. Fletcher, R. *Practical Methods of Optimization*; Wiley: Hoboken, NJ, USA, 2000.
28. Koroll, C. OJ:s Vågsystem—Belt Weigher Solutions. Available online: https://www.vagsystem.se/en/ (accessed on 28 June 2021).